ELECTROCHEMISTRY

Approaching high-performance potassium-ion batteries via advanced design strategies and engineering

Wenchao Zhang[1,2]*, Yajie Liu[1]*, Zaiping Guo[1,2]†

Potassium-ion batteries (PIBs) have attracted tremendous attention due to their low cost, fast ionic conductivity in electrolyte, and high operating voltage. Research on PIBs is still in its infancy, however, and achieving a general understanding of the drawbacks of each component and proposing research strategies for overcoming these problems are crucial for the exploration of suitable electrode materials/electrolytes and the establishment of electrode/cell assembly technologies for further development of PIBs. In this review, we summarize our current understanding in this field, classify and highlight the design strategies for addressing the key issues in the research on PIBs, and propose possible pathways for the future development of PIBs toward practical applications. The strategies and perspectives summarized in this review aim to provide practical guidance for an increasing number of researchers to explore next-generation and high-performance PIBs, and the methodology may also be applicable to developing other energy storage systems.

INTRODUCTION

Developing high-performance lithium-ion batteries (LIBs) is vital for regulating the energy output of intermittent solar and wind energy, which have been expected to occupy increasing proportions of energy sources in light of the environmental issues caused by fossil fuel energy (*1*–*3*). Because of the limitations imposed by lithium's rarity [0.0017 weight % (wt %)], its uneven distribution in Earth's crust, and its high cost, LIBs cannot meet the demand for energy storage devices with low cost, high energy density, long cycle life, and fast charging/discharging capabilities (*1*, *2*). Sodium-ion batteries (SIBs) have attracted great attention as a promising alternative to LIBs because of sodium's high abundance and low cost (*3*). Nevertheless, the inherent properties of Na-ion chemistry originating from its high standard reduction potential [−2.71 V versus standard electrode potential (E^0)] strongly limit the energy density of SIBs, which makes them unacceptable for some practical applications such as electric vehicles (*4*).

The motivations triggering the study of potassium-ion batteries (PIBs) relate to the benefits of their relatively high energy density resulting from the low standard reduction potential of potassium (−2.93 V versus E^0), which is close to that of lithium (−3.04 V versus E^0) (Fig. 1A) (*4*); their low cost, which is ascribed to the abundance of potassium (1.5 wt %) (*5*) in Earth's crust (Fig. 1B); and also their fast ion transport kinetics in electrolyte. The price of potassium metal is relatively high compared with sodium; however, the price of potassium salt, i.e., the raw materials for electrode fabrication (K_2CO_3), is similar to that of Na_2CO_3, which is much cheaper compared to Li_2CO_3. In addition, aluminum foil can be used as a current collector in PIBs instead of the copper foil found in LIBs, which will not only notably reduce the price of the PIB but also reduce the weight of the current collector and address over-discharge problems (*6*). Although potassium has the largest atomic radius (1.38 Å) compared to lithium (0.68 Å) and sodium (0.97 Å), K^+ has the smallest Stokes' radius (3.6 Å) compared to Li^+ (4.8 Å) and Na^+ (4.6 Å) in propylene carbonate (PC) solvents (Fig. 1C) (*7*), indicating that it has the highest ion mobility and ion conductivity. In addition, it has been proven that the diffusion coefficient of K^+ is about three times larger than that of Li^+, as investigated by ab initio molecular dynamics simulations (MDS) (*8*). On the basis of the advantages mentioned above, replacing Li^+ with K^+ would enable us to enhance the rate capability and realize high mass loading electrodes without sacrificing specific capacity.

Recently, we have witnessed an astounding increase in publications regarding PIBs (Fig. 1D). Growing research efforts have been devoted to understanding the electrochemistry of PIBs and improving and achieving high electrochemical performance with various strategies based on the design and development of electrode materials, electrolyte, and electrode/battery configurations. Specifically, the strategies involved, such as nanostructured design, the use of a conductive matrix, heteroatom doping, electrolyte optimization, and/or electrode design, play important roles in many aspects, such as manipulating the interfacial reactions, alleviating volume variations, regulating electronic structures, and avoiding excessive side reactions. This Review attempts to highlight (i) the key issues that are hindering the future development of PIBs, (ii) recent strategies and advances in achieving high-performance PIBs, and (iii) possible directions and avenues for targeting low-cost, long-life, safe, and fast-charging/discharging PIBs. Our main objective is to illustrate specific strategies for developing PIBs, provide possible directions for the future development of next-generation PIBs, and suggest methodologies for the development of other energy storage devices.

CHALLENGES OF PIBS

High–energy density electrodes need to be developed to guarantee high energy output, and structural stability should be maintained via material/electrode design to ensure long cycling performance. To achieve high energy density and high cycling stability in PIBs, their interfacial chemistry, ion diffusion in solid electrodes, electrolyte functions, and the correlations among them need to be deeply

[1]Institute for Superconducting and Electronic Materials, Australian Institute for Innovative Materials, University of Wollongong, Innovation Campus, North Wollongong, NSW 2500, Australia. [2]School of Mechanical, Materials, Mechatronic, and Biomedical Engineering, Faculty of Engineering & Information Sciences, University of Wollongong, Wollongong, NSW 2522, Australia.
*These authors contributed equally to this work.
†Corresponding author. Email: zguo@uow.edu.au

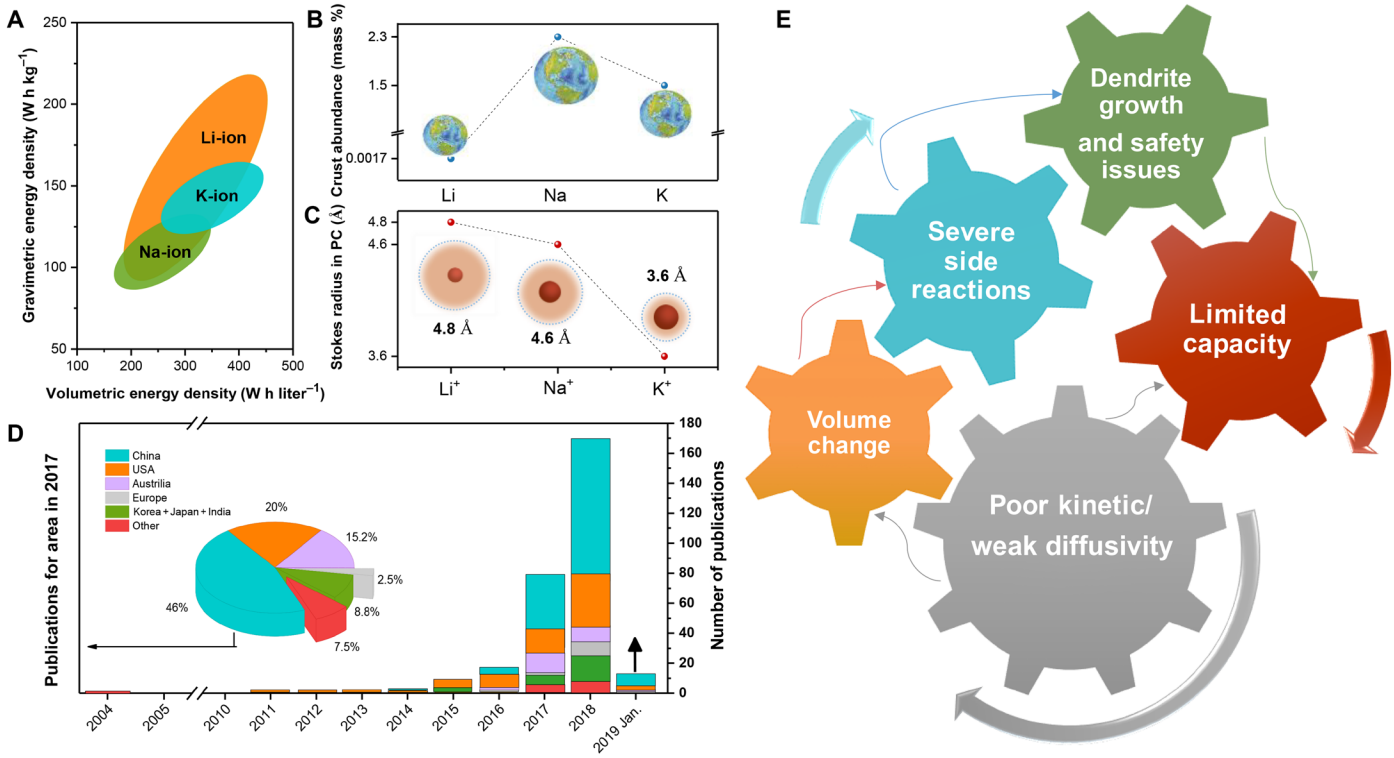

Fig. 1. Opportunities and challenges of the PIB. (**A**) Comparison of LIB, SIB, and PIB in terms of energy density. (**B**) Abundance of lithium, sodium, and potassium metal in Earth's crust (wt %). (**C**) Stokes radius of Li^+, Na^+, and K^+ in PC. (**D**) Number of publications on PIBs according to Google Scholar (as of January 2019). (**E**) Summary of challenges and their relationships for the PIB.

understood to properly address the main specific issues/challenges in potassium ion storage as shown below.

Low ion diffusivity in solid electrodes/poor K^+ reaction kinetics

The rate performance of PIBs not only is crucially dependent on the ion diffusion in the electrolyte but also relies on the ion diffusivity and electron transfer in solids. Although potassium has the weakest Lewis acidity and the smallest Stokes' radius, leading to fast ionic conductivity in the electrolyte, its poor ion diffusivity in solids could still constitute a limitation for the reaction kinetics due to the large atomic size of K^+ (*9*).

Large volume variations during potassiation/depotassiation

During cycling, the electrode materials undergo volume changes due to the insertion/extraction of K ions. It has been demonstrated that graphite has ~61% volume expansion after potassiation, which is six times larger compared to that after lithiation (*10*). The high–theoretical capacity alloy/conversion-based anodes undergo a much greater volume change during cycling [~400% for Sb_2S_3 and ~681% for Sn_4P_3; (*11*)]. Such huge volume changes in the continuous cycling process undoubtedly result in pulverization and create some "dead" areas, which are electrically isolated from the conductive agents and cause capacity fading (*12*).

Severe side reactions and consumption of electrolytes

Owing to the low electrochemical potential of K^+/K, the solvent in the electrolyte could be readily reduced on the electrode surface (*13*). It was reported that cells cycled to a lower cutoff voltage exhibited relatively lower initial coulombic efficiency, indicating that more side reactions occur with the lower cutoff voltage. The severe side reactions will further consume the electrolyte and cause drying out of the electrolyte after a certain number of cycles, leading to a sharp increase in polarization and causing degradation of the electrode capacity (*11*).

Dendrite growth

K dendrite growth should be taken seriously in the research of PIBs, as well as for other novel battery systems [K-S (*14*), K-Se (*15*), and K-O_2 (*16*)], which directly apply potassium metal as anode. The plating and stripping electrochemistry of K metal and an uneven ion flux or electron distribution would lead to K deposition in dendritic form, which will induce safety concerns caused by the possibility of an internal short circuit.

Battery safety hazards

The battery safety is inherently threatened by the poor heat dissipation, and thermal runaway is considered to be the main issue that induces safety concerns. K has a lower melting point and more reactive characteristics compared to Li; thus, more attention needs to paid to PIBs to address such safety concerns. It was reported that the K-graphite system could go into thermal runaway at a lower temperature (100°C versus 150°C), but it would generate less heat compared to the commercial Li-graphite anodes (395 J g^{-1} versus 1048 J g^{-1}) (*17*). Safety issues related to thermal runaway are still complicated especially for the PIB system, which should be addressed from the aspects of electrode materials, electrolyte, cell configurations, etc.

Limited energy density/power density

As an alternative choice to LIBs, the energy density and power density of PIBs should be taken into consideration for future practical applications (*18*). Although PIBs have a higher operating voltage than SIBs, similar to that of LIBs, which may promote high energy density, the maximum energy density and power density are still limited owing to the large atomic mass of K and the sluggish reaction kinetics during insertion/extraction.

Understanding the correlations between the six main issues (Fig. 1E) is probably the most effective way to confront and address these problems. During cycling, the poor ion diffusivity in solid electrodes could lead to sluggish reaction kinetics, which affects the ion migration and rate capability of the batteries. In addition, the large volume variations during cycling could damage the integrity of the electrodes and cause pulverization, which may lead to further concerns about the severe side reactions due to the formation of the solid-electrolyte interphase (SEI) layer on the newly created surface. As far as the metal anode is concerned, the side reactions will be accelerated by the uneven electron distribution, which will lead to dendrite growth and thus the further fracturing of the SEI. The SEI layer will continuously form on the surface of the electrode, which will consume the electrolyte; further increases the polarization of the electrode; and results in capacity fading. All in all, the dendrite growth/safety issues, severe side reactions, unstable SEI film, low ion transportation, and large volume changes will eventually result in capacity fading and failure of the battery.

STRATEGIES APPLIED TO PIB DESIGN AND IMPROVEMENT

Nanostructural design and engineering for improving the K^+ reaction kinetics

Nanostructured electrodes advance with the development of nanotechnology, and great efforts have been made in nanostructure design with the aim of improving the electrochemical performance of metal-ion batteries (*19*). Considering the large size of K^+ in PIBs, the nanostructural design of electrode materials is one of the most effective ways to improve the K ion diffusivity/reaction kinetics by shortening the potassium ion diffusion length, thus enhancing their rate capability and cycling performance.

Nanostructured designs have been successfully applied for most anode materials and cathode materials such as carbon-based materials [graphite (*10*, *20*), hollow carbon (*21*), and graphene (*22*)], alloy-based electrodes (*11*, *23*), oxides (*24*), sulfides (*25*, *26*), selenides (*27*), and Prussian blue (PB) and its analogs (*28*–*30*) (Fig. 2). Several nanostructures have been studied for graphite, including polynanocrystalline (*20*) and nanocage (*31*) structures. Among them, a three-dimensional (3D) interconnected network structure could offer fast electron transfer capability due to its naturally high electrical conductivity and provide enough channels for ion transportation. Thus, highly graphitic carbon nanocages were proposed to effectively maintain the structural stability of the network during K^+ intercalation/deintercalation because the anisotropic cage-like structure could prevent interlayer slipping and ensure structural integrity, so that a high capacity retention of 79% at 35 C was achieved (*31*). In addition, the cycling stability of the electrodes was notably enhanced by replacing the graphite anode with other carbon-based anodes, including soft carbon, carbon nanotubes (CNTs), carbon nanospheres (*21*), and carbon nanofibers (*32*). Porous structures are attractive due to their high specific surface area, which could facilitate contact between the electrolyte and the active materials, thus improving the coulombic efficiency. In a recent study, a porous carbon nanofiber electrode was synthesized, and it exhibited excellent rate capability (101 mA h g^{-1} at 20 A g^{-1}) and promising long cycling stability (4000 cycles) (*32*). In addition to carbon-based materials, sulfur/selenium-based and alloy/conversion-based anode materials could be good candidates due to their high gravimetric and volumetric specific capacities. To date, nanoparticles (*33*), nanosheets (*25*), nanoroses (*34*), and nanoclusters (*26*) have been designed for VS_2, SnS_2, MoS_2, Sb_2S_3, CoS, and VSe_2. These designs can effectively alleviate the volume changes and improve the reaction kinetics to some extent for sulfur/selenium-based electrodes. Specifically, with the decreased thickness of the Sb_2S_3 nanosheets prepared by our group, the shortened ion diffusion pathways result in improved rate capability, especially at high current densities (*9*). Liu *et al.* reported $K_{0.6}MnF_{2.7}$ hollow nanocubes as zero-strain material for enhanced potassium storage with only 1.4% volume expansion and negligible lattice parameter change (<1%), which made it possible to deliver over 100 mA h g^{-1}, even after 10,000 cycles (*35*). Nanodesign for cathodes could also facilitate structural integrity and stability to some extent, thus enhancing the cycling performance and ensuring reversible intercalation/deintercalation of K^+. PB and its analogs with structures of nanoporous fibers, nanoparticles, and nanocubes have been widely used as cathode for PIBs because of their open framework with large interstitial spacing, which could allow fast ionic transportation. A detailed comparison of the electrochemical performance of crystallite-sized Prussian white was carried out by He *et al.*, demonstrating that the optimized cathode material with a particle size of 20 nm could deliver a close-to-theoretical reversible capacity of 140 mA h g^{-1} (*36*).

Although nanodesign could facilitate the K^+ reaction kinetics to some extent with enhanced electrochemical performance, high cost, low tap density, side reactions, and relatively high working voltage plateau due to surface capacitive behavior could be main challenges. From our perspective, several efficient ways could be used: (i) applying well-mixed nano- and microsized materials together in a certain ratio so that nanosized particles can effectively occupy the interspaces among the microsized particles; (ii) using active materials with a secondary structure, such as micro-nanostructures, to increase the pack density; (iii) using surface coating as a promising way to alleviate the undesirable surface reactions arising from the large surface area of nanomaterials; and (iv) further developing low-cost, simple, and automatic engineering fabrication techniques for nanomaterials, for example, improved exfoliation for large-scale nanosheet (*37*, *38*) production and automatic reactor systems for continuous and scalable production of nanocrystals (*39*).

Buffering volume changes and enhancing electrical conductivity by using a carbon matrix

The huge volume variations during electrochemical cycling are always the main issue for the failure of alloy-based (Sn, Sb, P, etc.) and sulfur/selenium-based anode, and this problem can be more serious in PIBs than in LIBs and SIBs due to the large atomic radius of potassium ions (*12*). To address this problem, an effective and straight forward strategy is to use a soft and conductive matrix to buffer the volume changes during potassiation/depotassiation processes (*40*).

As one of the most efficient and easily scaled-up production techniques, ball milling was widely used to obtain a carbon matrix for active materials in PIB electrode fabrication. Uneven distributions

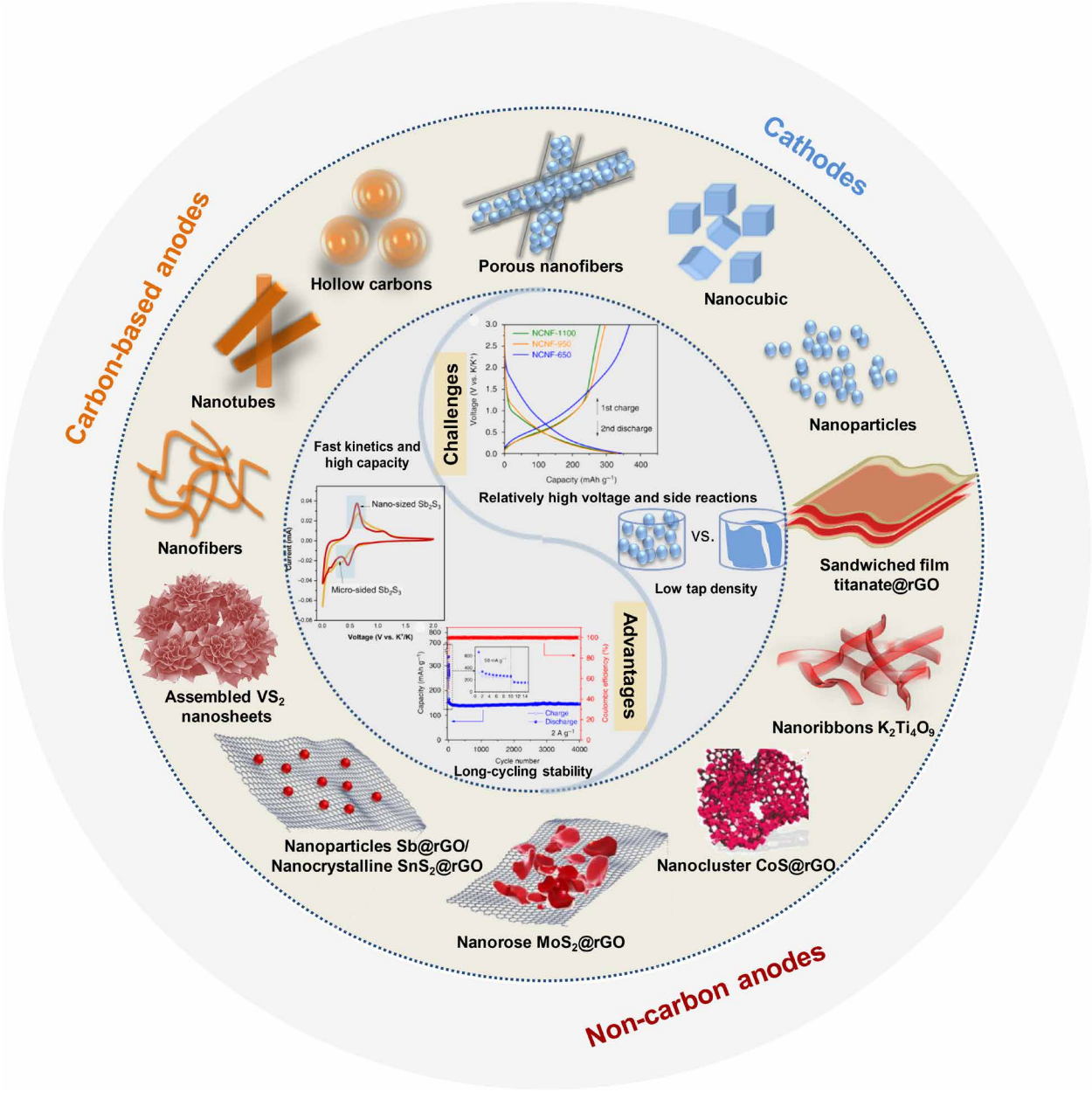

Fig. 2. Illustration of various structured electrodes that have been reported for the PIB with their advantages and challenges for nanoscale engineering. Inset figures are reproduced with permission from the Nature Publishing Group (*32*).

of carbon and relatively big particles from ball milling, however, cannot effectively solve the volume variation problem of electrodes during potassiation/depotassiation, leading to the limited cycling stability. The other ways of introducing a carbon matrix include hydrothermal, electrospinning, and solution-based chemical methods annealing from polymer and chemical vapor deposition. In terms of the electrospinning or solution-based fabrication method, although a uniform carbon distribution can be achieved, the complex synthesis process induces high production costs, and the solvents involved in the synthesis might introduce side-reaction products and impurities, decreasing the electrical conductivity of the electrode materials and thus lowering the coulombic efficiency of the batteries. In addition, amorphous carbon produced via high-shear exfoliation was demonstrated by our group (*9*). The carbon content from in situ carbonization during exfoliation is hard to control, however, and further investigations are required.

Various kinds of carbon-based matrix as a buffer for volume change of electrodes have been used such as graphite, hard carbon/soft carbon, doped carbon, CNT, and graphene (Fig. 3A). Amorphous carbon is easily fabricated with relatively low conductivity due to low carbonization temperature. Reduced graphene oxide (rGO) is a widely used benign carbon matrix owing to its excellent electrical conductivity and flexible 2D structure. In addition, the rational structural design of matrix and active material could promote the production of a uniform soft matrix. Inspired by the advantages of layer-by-layer structures (offering a stable scaffold for volume expansion

and an electrochemically protective layer by facilitating the formation of a stable SEI layer), a sandwich-type hybrid structure (MXene/rGO nanosheets) was fabricated to improve the rate performance and long cycling stability (*41*). In general, unique structural designs, such as surface coating to ensure effective contact between the active materials and the soft conductive matrix, and simple synthesis routes that avoid additional costs and impurities might be the solution for the production of uniform conductive buffering matrices for electrode materials. Moreover, the synergetic effect of various components and active phases with different reaction plateaus can possibly enable them to act as buffer matrices for each other.

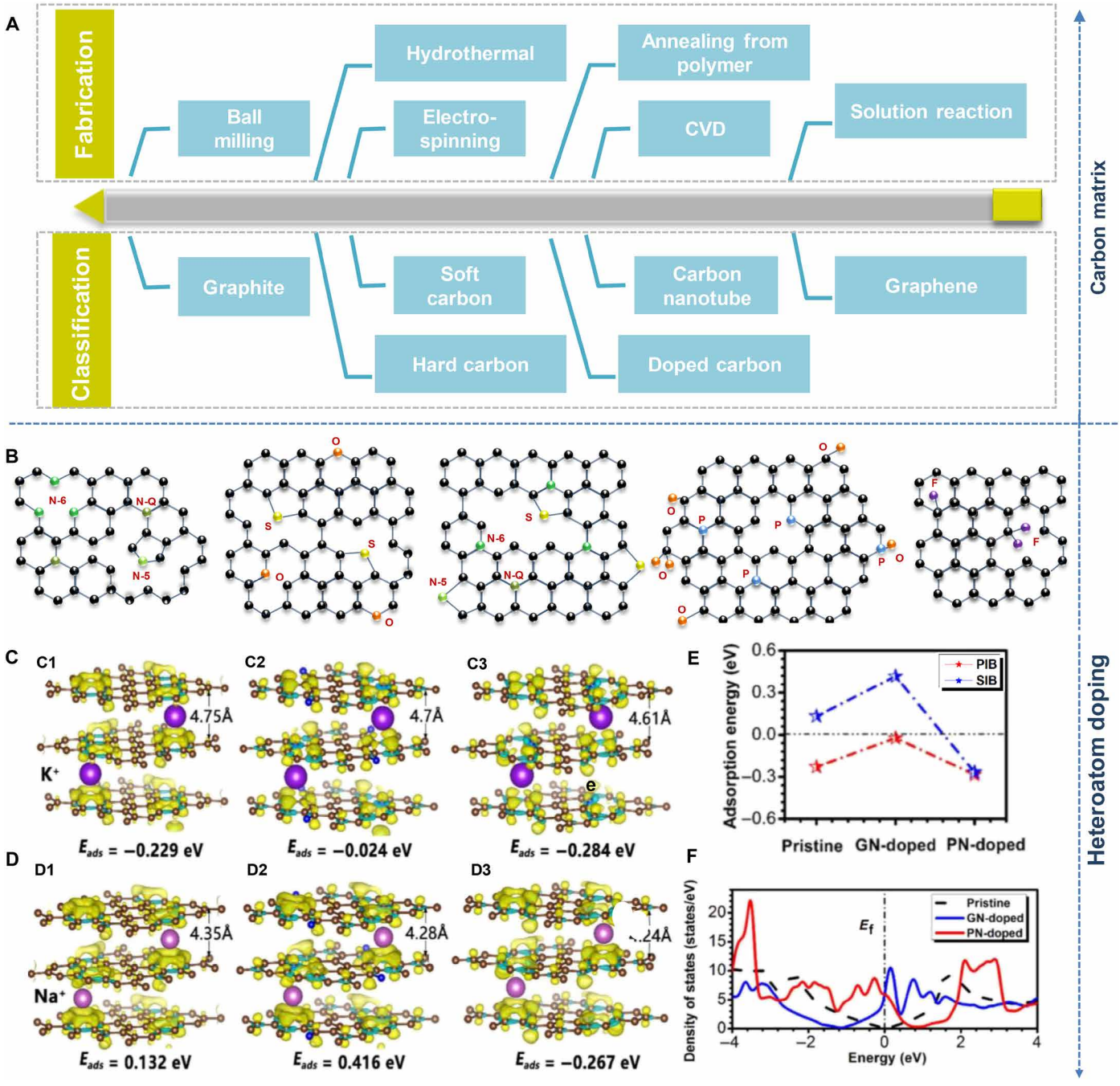

Fig. 3. Illustration and summary of strategies for employment of carbon matrix and heteroatom doping of electrodes. (**A**) Classification of carbon matrix materials for electrodes in PIBs with summary of the carbon matrix fabrication method. CVD, chemical vapor deposition. (**B**) Schematic illustration of reported doped carbon-based electrodes for the PIB. (**C** to **F**) Simulations of the K^+ and Na^+ adsorption capabilities and DOS of different carbon structures. (C1 to C3) Electronic density differences of K^+ ions adsorbed on pristine carbon, GN-doped carbon, and PN-doped carbon, respectively. Yellow areas represent +0.005 *e* per $Å^3$ isosurface; (D1 to D3) the electronic density differences of Na^+ ions adsorbed on pristine carbon, GN-doped carbon, and PN-doped carbon, respectively; (E) adsorption energies of K^+ and Na^+ ions on various sites; (F) DOS of different carbon structures (*44*). (C) to (F) are reproduced with permission from Elsevier (*44*).

Enhancing the kinetics via regulating the electronic structure and increasing the defects and vacancies by heteroatom doping

The heteroatom doping strategy for improving the reaction kinetics relies on the functions of the doping elements and tailorable features of the active materials (*42*, *43*). Doping was realized via heat treatment of organics and polymer precursors normally containing N (Fig. 3B) (*22*, *44*), S (*45*), P, or F (*46*) elements at high temperatures during the carbonization process. As for N doping, the isosurface plots of charge distribution and the adsorption energy of K/Na absorption on graphene are presented in Fig. 3 (C to E). It can be observed that the pyridinic N (PN) doping increases the amount of K–C bonds around the PN-doped site, while the graphitic N (GN) doping decreases the amount of K–C bonds in the carbon ring, indicating that GN doping leads to weaker K adsorption than in PN doping. The interaction between Na atoms and the nitrogen-doped carbon microsphere carbon structure is similar to that of K atoms. In addition, the density of states (DOS) results (Fig. 3F) suggest that the GN-doped sites are slightly electron rich, with a raised Fermi level compared to the undoped sites, thus leading to higher electronic conductivity (*44*). According to further investigations, the reversible capacity and cycling stability might be improved with an increased doping level of nitrogen (*32*). F doping could facilitate fast ion transportations by offering favorable bonding sites for potassium storage in the vicinity of residual F atoms. It is believed that F doping into a carbon source would be feasible due to the high electronegativity (χ = 3.98) of elemental F. On the basis of the density functional theory (DFT) calculations, the C–F covalent bonds that are formed could change the carbon hybridization state from sp^2 to sp^3, which provides high electrical conductivity and thermodynamic stability (*46*). Boron, as it has a similar atomic size to carbon, has been considered to be a potential doping element for carbon. Although no experimental results have been reported as yet, DFT calculations show that B-doped graphene has a large capacity (564 mA h g^{-1}), a smaller diffusion energy barrier, and less structural deformation in PIBs compared to SIBs (*47*).

Attempts have been extended to multiple-element doping [such as S/O-doped (*48*), N/O-doped (*49*), S/N-doped (*50*), and P/O-doped (*51*) carbon] (Fig. 3B). It was reported that doping oxygen into the carbon framework could improve the wettability by reducing the inert surface area and provide more active sites for enhancing the capacity. It reduces electrical conductivity, however, leading to poor cycling performance. To overcome this drawback, heteroatom N/O-codoping was successfully applied in hard carbon with demonstrated good cycling performance (*52*). When it comes to sulfur and phosphorus doping, the electron-donor properties of both of them cause the formation of structural defect sites or favorable spin densities throughout the carbon. P/O-codoped graphene electrodes were investigated, and they showed enhanced electrical conductivity and chemisorption of potassium ions (*51*). Besides, S/N-codoped graphene as a supporting matrix demonstrated high reactivity, strong affinity with the active material, good electrical conductivity, and robust stability (*50*).

Although various heteroatom doping strategies have been investigated in PIBs, further experimental work and in-depth discussion are needed to completely understand the correlation between structure/doping effects and their electrochemical properties. Furthermore, the doping level, doping sites, and doping depth need to be accurately characterized using advanced techniques.

Regulating salt chemistry and electrolyte additives to minimize side reactions and K dendrite growth

K-ion chemistries present more severe challenges to the electrolyte and interphase due to more dynamic changes in their electrode structures during cycling. Unsuitable electrolytes or additives could raise serious issues, including severe side reactions in the electrolyte or interphase, the creation of an unstable SEI layer during cycling, and potassium dendrite growth on the electrodes (Fig. 4A).

The stability of the SEI has an immediate impact on the cycling life, and it is considered as a challenge for the long-cycling performance of PIBs. Besides excellent ion conductivity and electron-blocking capability, researchers have concluded that the SEI on electrodes or K metal must be stable and needs to be homogeneous in composition, morphology, and ionic conductivity. It was found that the cycled Bi/rGO electrodes in the potassium bis(fluorosulfonyl)imide (KFSI) electrolyte had a higher surface potential than that in the KPF_6 electrolyte (Fig. 4, B and C), indicating higher conductivity compared to the electrodes cycled in the KPF_6 electrolyte (*53*). Also, in the KPF_6 electrolyte, more heterogeneous and thicker SEI layers were formed as cycling progressed, thus leading to continuous consumption of the electrolyte as compared to the KFSI electrolyte (*11*, *54*). In addition to the carbonaceous electrolytes [ethylene carbonate (EC), diethyl carbonate (DEC), and PC; (*36*, *55*)], ether-based electrolytes [dimethyl carbonate (DMC) (*56*), diglyme (*57*, *58*), dimmethoxyethane (DME) (*59*–*61*), and dimethyl sulfoxide (*62*)] have the excellent advantages of promoting stable SEI formation, maintaining high coulombic efficiency, facilitating strong chemical adsorption, and enhancing the charge-transfer kinetics (*23*, *63*). For example, the elastic and adhesive oligomer-containing SEI formed in diglyme-based electrolytes helps to achieve a Bi electrode with long cyclability and high coulombic efficiency (Fig. 4D) (*63*). Moreover, DME has a higher electron donation number than EC-DMC, making it much easier to interact with the K ions so as to modify the electrolyte-K^+ polarity and diffusivity for better kinetics (*61*).

Dendrite growth is considered to be one of the primary reasons for safety issues during cycling, and potassium more easily grows dendrites than lithium because of its reactivity (*57*). The KFSI-DME electrolyte as an efficient medium can passivate the K surface, enabling reversible K plating and stripping with the formation of a uniform and stable SEI layer (Fig. 4E) (*59*). Polymer electrolytes were chosen as a good candidate because of their good mechanical properties and the ease of processing inherent to plastic materials, providing substantial improvements to safety and electrochemical stability in PIBs when compared with conventional liquid electrolytes (*64*). A reported K[FSA]-[C_3C_1pyrr][FSA] (FSA = bis(fluorosulfonyl)amide; C3C1pyrr = *N*-methyl-*N*-propylpyrrolidinium) ionic liquid has been evaluated as electrolyte for PIBs and exhibited low viscosity and high ionic conductivity, which effectively suppressed dendrite growth, thus enhancing cycling stability (*65*).

Electrolyte additives represent another effective strategy to improve the electrochemical performance of energy storage devices, since fluoroethylene carbonate (FEC) has been demonstrated to assist the formation of a stable SEI layer during cycling in SIBs (*66*–*68*). However, Bi anode with 3 volume % FEC in the KPF_6/EC/PC electrolyte (*63*) and Sn_4P_3 anode with 5 wt % FEC in EC/DEC exhibited large polarization and fast capacity fading (*11*). In addition, potassium foil electrodes in the electrolyte with FEC additive showed higher hysteresis (±500 mV) than those without FEC (±200 mV) (Fig. 4F). However, FEC-based electrolytes are more attractive for high-voltage electrodes. $K_{1.92}Fe[Fe(CN)_6]_{0.94}$ cathode with 2% FEC additive in the

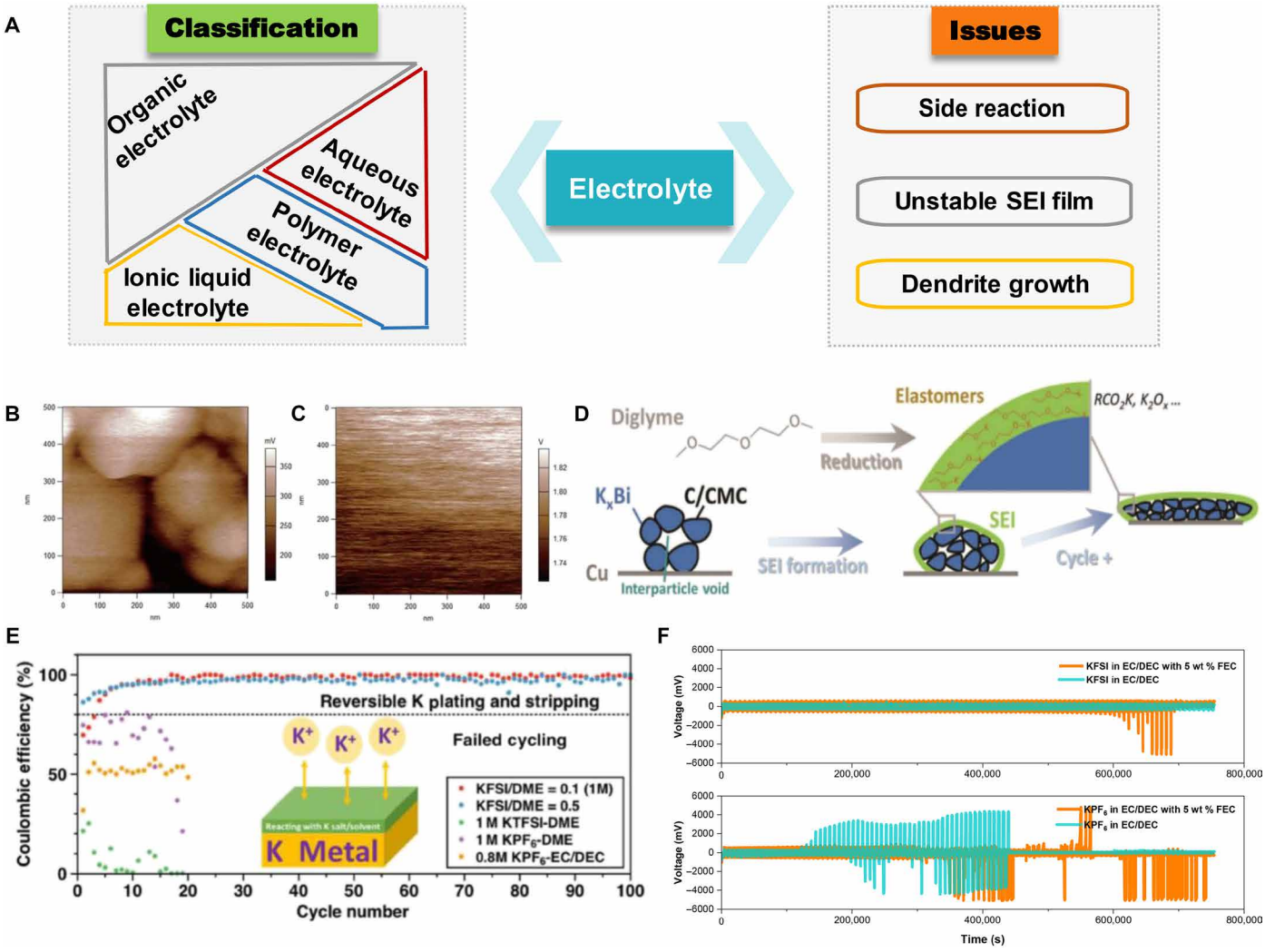

Fig. 4. Classification and summary of electrolyte engineering strategy. (**A**) Using various electrolytes (or regulating electrolyte salts and solvents) to overcome the related issues of side reactions, unstable SEI film, and dendrite growth. Surface potential maps of the Bi/rGO electrode for (**B**) the KPF_6 electrolyte and (**C**) the KFSI electrolyte. (B) and (C) are reproduced with permission from John Wiley and Sons (*53*). (**D**) Schematic illustration of the morphology changes and SEI formation in the electrochemical processes with diglyme-based electrolytes. Reproduced with permission from John Wiley and Sons (*63*). (**E**) Comparing galvanostatic K plating and stripping on the Cu substrate in different electrolyte formulations at a rate of 0.05 mA cm^{-2}. Reproduced with permission from the American Chemical Society (*59*). (**F**) Comparing the cycling performances of cells with various electrolytes (with or without FEC) at 50 mA g^{-1}. Reproduced with permission from Elsevier (*11*).

EC/DEC electrolyte in the voltage range of 2.0 to 4.3 V could exhibit enhanced initial coulombic efficiency from 60% (without FEC additive) to 90% (*60*). In summary, FEC as an electrolyte additive in PIBs could stimulate electrolyte decomposition/side reactions under low voltage potential (<2.0 V), while FEC may reduce the polarization and interfacial resistance to some extent and increase the initial coulombic efficiency in relatively high voltage ranges (>3.0 V).

Fracturing of the SEI layer, in conjunction with further chemical side reactions and fast dendrite growth, will eventually lead to both safety hazards and fast capacity fading of batteries. There is a great necessity to further characterize the transformations of the SEI layer and identify the electrolyte decomposition products in various electrolytes using various advanced techniques, which will be valuable for a deep understanding of SEI formation and will help in optimizing electrolytes. The electrolyte additives, even with content only at the parts-per-million level, can alter the uniformity, composition, and even mechanical properties of the SEI, notably influencing the cycling stability of electrodes.

Enhancing the energy density by electrode design

The electrode design is well developed with the aim of decreasing manufacturing costs, increasing the utilization of active materials, and, thus, increasing the energy density of batteries. Conventional electrodes fabricated by a slurry casting onto metal foil cannot maintain structural integrity during repeated mechanical deformation due to the weak adhesion between the current collectors and the active materials (*28*). Advanced flexible electrodes (normally current collector–free flexible electrodes), as an alternative option, not only notably reduce the electrode weight, thus increasing the energy density of cells, but also facilitate the development of flexible electronics (such as wearable devices). Few attempts have been made to create current collector–free flexible electrodes for PIBs to achieve low-cost, flexible,

and high–energy density electrodes. Simple pencil drawing on filter paper was used to fabricate a flexible anode, demonstrating nearly 200% capacity improvement due to this electrode design (Fig. 5A) (*69*). Recently, MXene with rGO nanosheets constructed in a sandwich structure in which the layers were close to each other was directly used as anode for PIBs (Fig. 5B) (*41*). PB nanocubes were grown on Xuan paper via cyanotype technology, and the discharge capacity of the flexible full cells remained almost unchanged, even when they were intentionally bent and folded during cycling (*28*). The abovementioned flexible electrodes showed very good mechanical strength, high cycling stability, and high energy density, which is very encouraging for future research on flexible batteries or devices.

Novel K-based systems were designed to pursue high energy/power density and safe PIB batteries

To directly use the potassium (K) metal as anode, ensuring a much higher energy density, extended systems such as K-S (*14*, *70*–*72*), K-O_2 (*16*, *57*, *73*, *74*), K-Se (*15*), and K-I_2 (*75*) have emerged. In the case of K-S/K-Se batteries (Fig. 5, C and D), Zhao *et al.* reported pioneering work on room temperature K-S batteries with the conversion-type reaction mechanism ($2S + 2\ K^+ \leftrightarrow K_2S_3$) (*14*). A different type of K-S battery based on solution-phase potassium polysulfide (K_2S_x) catholyte and hard carbon as anode was also demonstrated, and the proposed K-S battery could effectively address various issues, including the high reactivity of the potassium metal anode and the slow reaction kinetics of the solid sulfur (*71*). As for mechanism studies, Zou *et al.* reported the asymmetric nature of the discharge/charge behavior of PIBs, which may be due to the weak solvation energy and strong cation-anion electrostatic interaction between K^+ and S_x^{2-} (*76*). Yu and Manthiram rationally designed a cathode separator by coating single-wall CNTs on Celgard to improve the utilization of sulfur active materials and enhance the cycle life of the K-S battery (*77*). K-O_2 batteries feature a high theoretical capacity and an abundant oxygen resource. The mechanism of K-O_2 batteries is to use K^+ to capture O_2^- and thermodynamically form electrochemistry and chemical stability of KO_2 as the reaction product (*16*). K-O_2 batteries with KPF_6 in ether-based electrolyte can be operated with low overpotentials, and a highly reversible single-electron transfer process was demonstrated by quantifying trace amounts of its side products (Fig. 5E) (*78*). A K-I_2 battery was investigated with highly reversible conversion among I_2, KI_3, and KI, and a capacity retention of 79% could be achieved after 500 cycles (*75*). Nevertheless, the heavy mass of the I_2 electrode compromises the output capacity of metal-based batteries (156 mA h g^{-1}), which limits its applications.

With nonflammable properties and high rate capabilities, aqueous-based battery systems exhibit great potential in large-scale electric grid applications with barely any safety concerns compared to the organic electrolyte systems (*79*). For PIBs, a nickel hexacynoferrate electrode was evaluated in 1 M KNO_3 electrolyte, and the cell showed superior rate capability and round trip energy efficiency (*29*), although the capacity, which relies on the one-electron Fe III/II process, was below 70 mA h g^{-1}. On the basis of the PB analogs, Su *et al.* reported a potassium-rich iron (II) hexacyanoferrate electrode, which can supply two electrons per formula unit and deliver exceptionally high capacity (up to 120 mA h g^{-1}) with high reversibility over 500 cycles (Fig. 5F) (*80*) A specific energy of ~65 W h kg^{-1} and a specific power of 1250 W kg^{-1} were achieved (Fig. 5G) (*80*). Even so, a narrow operating voltage window is another limitation for the aqueous PIB. To address this problem, finding a suitable electrolyte for the aqueous-based battery does matter. By using a potassium acetate–based water-in-salt electrolyte, the $KTi_2(PO_4)_3$ electrode showed reversible redox behavior and could provide a potential window of 3.2 V, which extends the avenue for exploration of high-energy-density aqueous PIBs (*81*).

Potassium-based dual-ion batteries (DIBs) operate on the basis of the intercalation/deintercalation of both cations (K^+) and anions (PF_6^- or FSI^-) into/out of electrodes (Fig. 5H), aiming to fabricate low-cost, high–energy density, environmentally friendly batteries (*82*–*84*). Several potassium-based DIBs have been reported, such as a potassium-based battery–supercapacitor hybrid device (*81*), a battery using metal foil as anode and expanded graphite as cathode (*83*), a symmetric $K_2NiFe^{II}(CN)_6$ cell (*85*), and graphite symmetric cells (*86*). The intercalation/deintercalation mechanism of anions in traditional graphite cathode requires high voltage, however, which will result in severe decomposition of the traditional electrolyte. By adopting some expensive ionic liquid–based electrolytes (*82*) or applying organic electrodes with relatively lower working voltage, the DIBs show comparatively high gravimetric energy density and excellent cycling stability, which could possibly meet the requirements of high–operating voltage and high–power density devices.

Using theoretical DFT calculations to predict the most desirable electrode materials with enhanced reaction kinetics and gain insight into the electrochemical mechanism

To gain insight into and a deep understanding of K-ion chemistry to address the critical issues mentioned above and reveal/explain the results from experiments, theoretical DFT calculations play an important role in PIB research (*87*, *88*). DFT calculations could be used to predict some potential electrode materials for PIBs. In the early research, it was predicted that hexagonal BC_3 could have potential theoretical capacity with the formation of $K_{1.5}BC_3$, and B-doped graphene potentially shows large capacity and high rate performance (*47*). In the case of the C_3N monolayer (with a high storage capacity of 1072 mA h g^{-1}), the low diffusion barrier energy (0.07 eV) for K on the C_3N monolayer surface implies high mobility and high rate capability for batteries (*89*). Besides, first-principles calculations help in obtaining a deep understanding of the physicochemistry properties of electrode materials, phase transitions during cycling, electrochemistry, the diffusivity of ion kinetics, and solvation structure. By calculating the K ion diffusion barrier (Fig. 5I), 1D diffusion pathway provided low diffusion barriers for K ion, indicating that the $KVOPO_4$ is a promising high-rate cathode material for PIBs (*87*). In conjunction with in situ x-ray diffraction (XRD), DFT calculations were used to unravel the phase transitions of Bi anodes ($Bi \rightarrow KBi_2 \rightarrow K_3Bi_2 \rightarrow K_3Bi$) during potassiation, and the volume expansion can be calculated on the basis of the crystalline parameters from in situ XRD data (*63*). As for electrolyte, first-principles MDS have been applied to reveal the solvation structure and dynamic properties (Fig. 5J) (*8*).

Although computational studies based on first-principles calculations provide very valuable metrics regarding solvation, diffusion energy barriers, interfacial kinetics, adsorption capability for K ions, etc., further calculations are still needed to gain a deep understanding of the electrochemical behavior and physicochemical properties of the electrodes, electrolytes, and electrode/electrolyte interfaces to achieve high-performance PIBs and facilitate their real application.

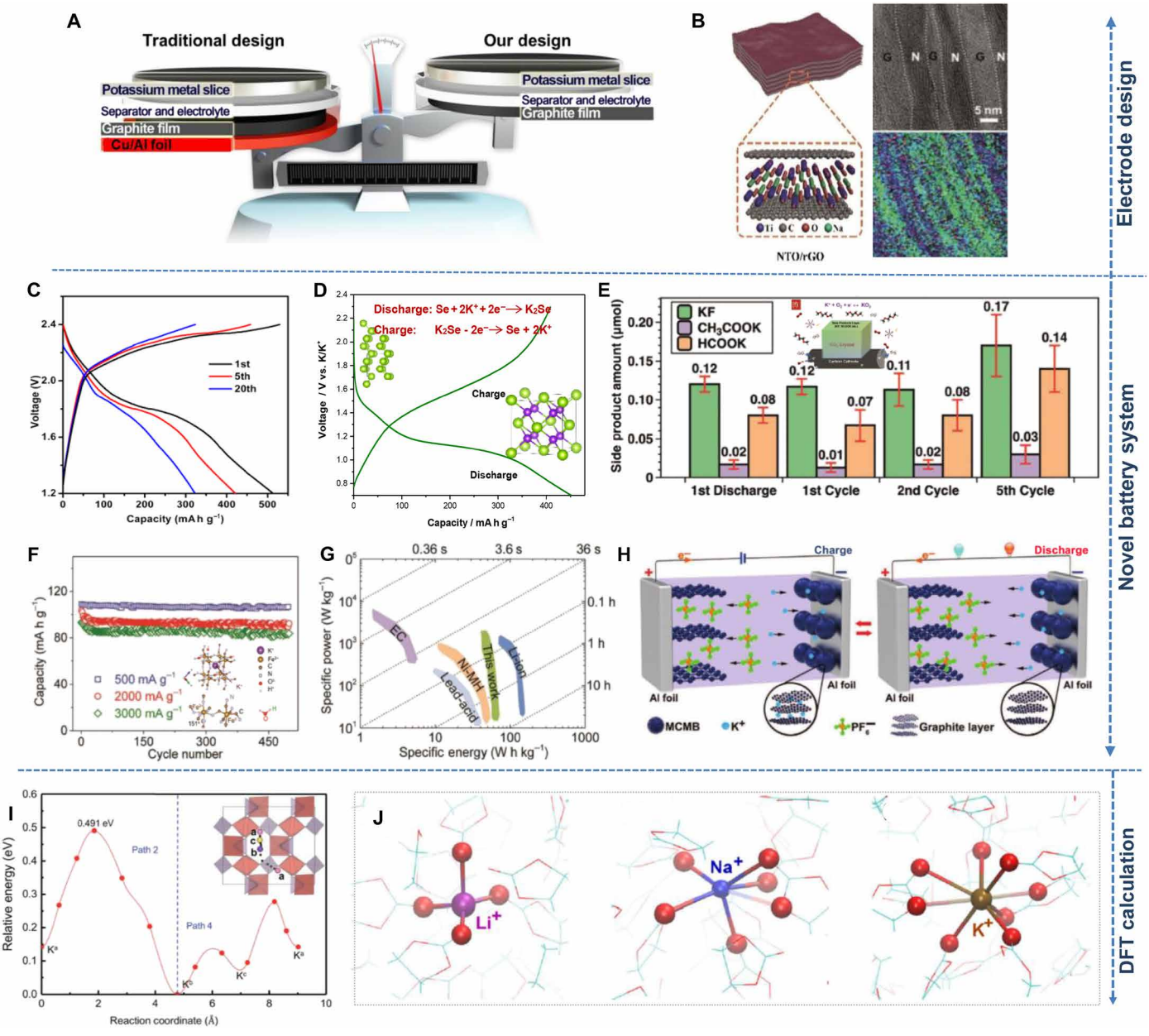

Fig. 5. The strategies of electrode design, novel K-based systems, and theoretical calculations for high-performance PIBs. (**A**) Schematic illustration of the special ultralight electrode design compared with a traditional electrode. Reproduced with permission from Elsevier (*69*). (**B**) Illustration showing the construction of flexible sodium titanate (NTO)/rGO films and high-resolution transmission electron microscopy images (with "N" referring to NTO and "G" referring to rGO), with the transmission electron microscopy elemental mapping images indicating the sandwich structures. Reproduced with permission from John Wiley and Sons (*41*). (**C**) Galvanostatic discharge–charge profiles of CMK-3/sulfur composite electrode at 50 mA g^{-1}. Reproduced with permission from Elsevier (*14*). (**D**) Charge/discharge profiles of the c-PAN-Se electrode at 0.2 C (PAN, polyacrylonitrile). Reproduced with permission from the American Chemical Society (*15*). (**E**) The amounts of side products on cycled electrodes collected at different stages (from left to right: KF, CH_3COOK, and HCOOK, with the SD calculated on the basis of three parallel cells). Reproduced with permission from John Wiley and Sons (*78*). (**F**) Charge and discharge capacities versus cycle number at current densities of 500, 2000, and 3000 mA g^{-1}, and (**G**) specific energy versus specific power for $K_2FeII[FeII(CN)_6]\cdot 2H_2O$–based aqueous PIBs, as well as several other devices: electrochemical capacitors (EC), lead-acid batteries, nickel metal-hydride batteries (Ni-MH), and LIBs. (F) and (G) are reproduced with permission from John Wiley and Sons (*80*). (**H**) Schematic illustration of the charging/discharging mechanism of the dual-carbon battery based on a potassium ion–containing electrolyte. Reproduced with permission from John Wiley and Sons (*100*). (**I**) Diffusion energy curve of $K_{1/16}VOPO_4$. The inset drawing shows the K ion diffusion pathways in $K_{1/16}VOPO_4$ (*87*). Reproduced with permission from the Royal Society of Chemistry (*87*). (**J**) Typical solvation structures of Li^+, Na^+, and K^+ in EC, indicating that the larger Na^+ and K^+ ions show more disordered and flexible solvation structures (*8*). Reproduced with permission from the American Chemical Society (*8*).

SUMMARY AND OUTLOOK

PIBs have attracted considerable interest, and a large number of electrode materials have been developed with reasonable electrochemical performance (Fig. 6). Although pioneering studies have been conducted to develop high-performance PIBs, we believe that notable advances still wait to be discovered to meet the requirements of practical applications. Herein, we outline several possible directions for advanced PIB research and hope that our perspectives may be useful for researchers in the field of PIB research.

Developing advanced electrode materials

Compared with amorphous carbon electrodes, the graphitic carbon electrode is promising for commercial applications because of its long and stable K^+ intercalation/deintercalation plateau above 0.1 V versus K^+/K, avoiding safety concerns and guaranteeing a high working voltage and high energy density. Further investigation should consider graphitic carbon anode to explore suitable graphitic microstructures with long stable cyclability as well as high tap density for commercial application.

Non-carbonaceous anode materials, especially the alloy-based electrodes, can be considered as alternatives for the development of electrodes with both high gravimetric and high volumetric energy density. Lamination of the electrode materials may be a good choice, which could not only buffer the volume variations but also enhance the conductivity. In the future, layered materials could be incorporated into multifunctional hosts, such as other 2D materials with enough wettability space for the electrolyte to enhance their electrochemical performance and increase the pack density.

As for cathode materials, energy density is a key parameter, which depends not only on the working plateau but also on the specific capacity (*90*, *91*). Generally, representative cathodes include conversion and insertion cathodes. In the case of insertion cathodes, K^+ can be inserted into and removed from the host matrix reversibly. Several compounds such as layered, spinel, olivine-type, and metal chalcogenides are worth applying as cathode for PIBs. The research on PIB cathodes is still at an early stage, and some representative Co- and Mn-containing transition metal oxides with potassium, such as $K_{0.5}MnO_2$ and $K_{0.6}CoO_2$, have been studied, but maintaining their structural stability during cycling is still a challenge (*92*). In addition, PB and its analogs are still the most popular and promising cathode materials owing to their open 3D framework, which is preferable for reversible electrochemical insertion/extraction of large alkali-metal ions such as K^+. Nevertheless, their limited capacity still hinders their real application. Further investigation of multi-electron storage per formula unit based on this 3D framework could be a promising research direction for developing cathode materials with high stability and high capacity.

In terms of conversion-type cathodes, they always undergo solid-state redox reactions accompanied by the breaking and reforming of chemical bonds during cycling. Fluorine and chlorine compounds, sulfur, and selenium-based composites are attractive owing to their high theoretical capacity and volumetric capacities (*91*). Studies of metal fluorides and chlorides, sulfur, and selenium-based cathodes have still been limited, however, due to their poor electrical conductivity, possible severe side reactions, and polysulfide dissolution, which limit their cycling stability. Development of a suitable electrolyte is a key approach, which deserves more attention to prevent polysulfide dissolution, improve the long-term cycling stability, and suppress the dendrite growth. In addition, oxygen could be a promising candidate as cathode in K-O_2 batteries, not only because of its high energy density but also because of its small polarization. Polymer-based or organic electrode materials have been studied to obtain low-cost and safe batteries, although further research needs to be conducted on the underlying mechanism and the reversibility of K ion insertion/extraction in polymer or organic systems.

Electrolyte optimization

We emphasize that the electrolyte should take first priority for the development of high-performance PIBs. Several criteria need to be met for the electrolytes to be effective: (i) they must be helpful for

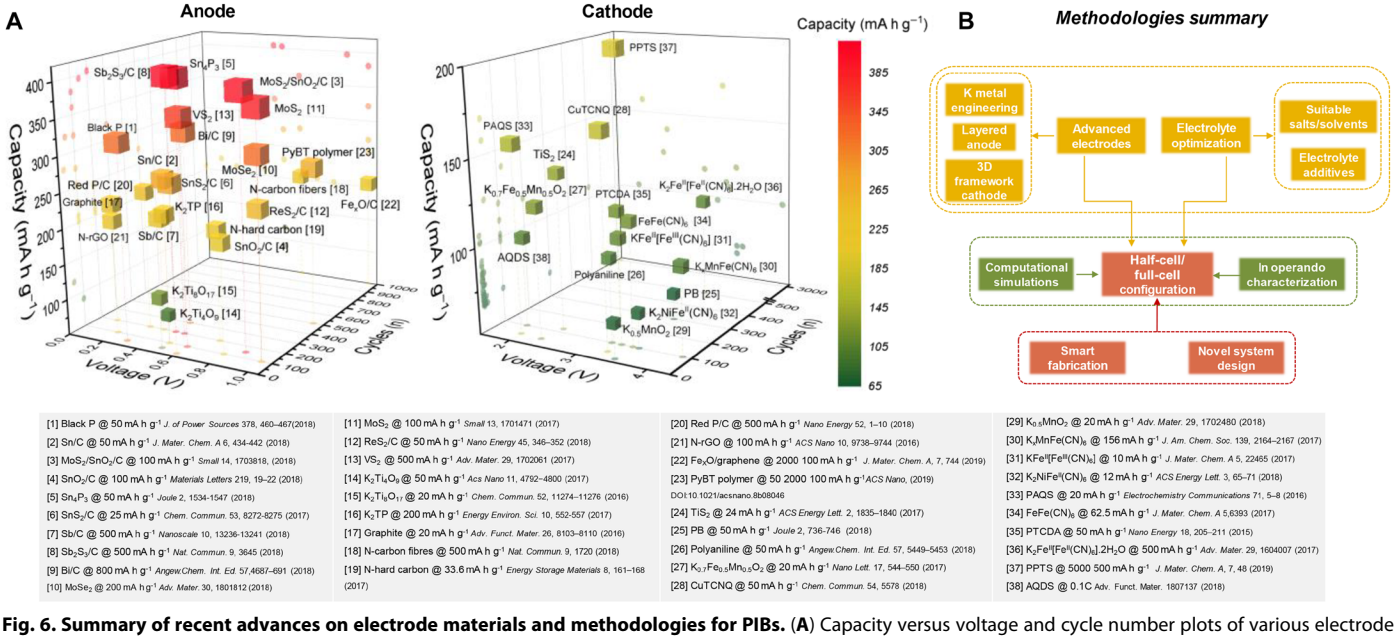

[1] Black P @ 50 mA h g^{-1} *J. of Power Sources* 378, 460–467(2018)
[2] Sn/C @ 50 mA h g^{-1} *J. Mater. Chem. A* 6, 434-442 (2018)
[3] MoS_2/SnO_2/C @ 100 mA h g^{-1} *Small* 14, 1703818, (2018)
[4] SnO_2/C @ 100 mA h g^{-1} *Materials Letters* 219, 19–22 (2018)
[5] Sn_4P_3 @ 50 mA h g^{-1} *Joule* 2, 1534-1547 (2018)
[6] SnS_2/C @ 25 mA h g^{-1} *Chem. Commun.* 53, 8272-8275 (2017)
[7] Sb/C @ 500 mA h g^{-1} *Nanoscale* 10, 13236-13241 (2018)
[8] Sb_2S_3/C @ 500 mA h g^{-1} *Nat. Commun.* 9. 3645 (2018)
[9] Bi/C @ 800 mA h g^{-1} *Angew.Chem. Int. Ed.* 57,4687–691 (2018)
[10] $MoSe_2$ @ 200 mA h g^{-1} *Adv. Mater.* 30, 1801812 (2018)
[11] MoS_2 @ 100 mA h g^{-1} *Small* 13, 1701471 (2017)
[12] ReS_2/C @ 50 mA h g^{-1} *Nano Energy* 45, 346–352 (2018)
[13] VS_2 @ 500 mA h g^{-1} *Adv. Mater.* 29, 1702061 (2017)
[14] $K_2Ti_4O_9$ @ 50 mA h g^{-1} *Acs Nano* 11, 4792–4800 (2017)
[15] $K_2Ti_8O_{17}$ @ 20 mA h g^{-1} *Chem. Commun.* 52, 11274–11276 (2016)
[16] K_2TP @ 200 mA h g^{-1} *Energy Environ. Sci.* 10, 552-557 (2017)
[17] Graphite @ 20 mA h g^{-1} *Adv. Funct. Mater.* 26, 8103–8110 (2016)
[18] N-carbon fibres @ 500 mA h g^{-1} *Nat. Commun.* 9, 1720 (2018)
[19] N-hard carbon @ 33.6 mA h g^{-1} *Energy Storage Materials* 8, 161–168 (2017)
[20] Red P/C @ 500 mA h g^{-1} *Nano Energy* 52, 1–10 (2018)
[21] N-rGO @ 100 mA h g^{-1} *ACS Nano* 10, 9738–9744 (2016)
[22] Fe_2O/graphene @ 2000 100 mA h g^{-1} *J. Mater. Chem. A*, 7, 744 (2019)
[23] PyBT polymer @ 50 2000 100 mA h g^{-1}*ACS Nano*, (2019) DOI:10.1021/acsnano.8b08046
[24] TiS_2 @ 24 mA h g^{-1} *ACS Energy Lett.* 2, 1835–1840 (2017)
[25] PB @ 50 mA h g^{-1} *Joule* 2, 736-746 (2018)
[26] Polyaniline @ 50 mA h g^{-1} *Angew.Chem. Int. Ed.* 57, 5449–5453 (2018)
[27] $K_{0.7}Fe_{0.5}Mn_{0.5}O_2$ @ 20 mA h g^{-1} *Nano Lett.* 17, 544–550 (2017)
[28] CuTCNQ @ 50 mA h g^{-1} *Chem. Commun.* 54, 5578 (2018)
[29] $K_{0.5}MnO_2$ @ 20 mA h g^{-1} *Adv. Mater.* 29, 1702480 (2018)
[30] $K_2MnFe(CN)_6$ @ 156 mA h g^{-1} *J. Am. Chem. Soc.* 139, 2164–2167 (2017)
[31] $KFe^{II}[Fe^{II}(CN)_6]$ @ 10 mA h g^{-1} *J. Mater. Chem. A* 5, 22465 (2017)
[32] $K_2NiFe^{II}(CN)_6$ @ 12 mA h g^{-1} *ACS Energy Lett.* 3, 65–71 (2018)
[33] PAQS @ 20 mA h g^{-1} *Electrochemistry Communications* 71, 5–8 (2016)
[34] $FeFe(CN)_6$ @ 62.5 mA h g^{-1} *J. Mater. Chem. A* 5,6393 (2017)
[35] PTCDA @ 50 mA h g^{-1} *Nano Energy* 18, 205–211 (2015)
[36] $K_2Fe^{II}[Fe^{II}(CN)_6].2H_2O$ @ 500 mA h g^{-1} *Adv. Mater.* 29, 1604007 (2017)
[37] PPTS @ 5000 500 mA h g^{-1} *J. Mater. Chem. A*, 7, 48 (2019)
[38] AQDS @ 0.1C *Adv. Funct. Mater.* 1807137 (2018)

Fig. 6. Summary of recent advances on electrode materials and methodologies for PIBs. (**A**) Capacity versus voltage and cycle number plots of various electrode materials for PIBs reported to date (as of January 2019). (**B**) Summary of methodologies in PIB research.

forming a uniform and stable SEI layer, (ii) they must be chemically stable with no decomposition in the operating voltage window, and (iii) they must be able to suppress excessive side reactions. Considering the progress on electrolyte additives and alternative potassium salt research, we believe that a low-fluoride potassium salt and an electrolyte additive could facilitate an even and stable SEI layer, avoid excessive side reactions, and suppress dendrite growth. Except for the wide use of FEC as additive, with successful experience in Li metal anode study, strategies such as using $LiNO_3$ and $AlCl_3$ to increase the interfacial stability, suppress dendrite growth, and help form a uniform SEI layer may offer new pathways for the exploration of suitable electrolyte additives for PIBs (*92*, *93*). It is also interesting to study alternative polymer-based electrolytes for PIBs since polymer-based electrolyte could suppress dendrite growth, avoid excess side reactions (*94*), and have better shape flexibility. Ether-based electrolytes are more favorable for batteries that need to have high cycling stability, and high salt concentrations have offered a possible route to the safe operation of potassium metal anodes. It has been challenging, however, to obtain solid evidence from characterizations of cycled cells, which makes it hard to unravel the roles of each salt and solvent in the electrolyte. Thanks to the in situ techniques developed recently, such as in situ Raman spectroscopy, cryogenic electron microscopy (*95*), and Fourier transform infrared microscopy, it is now possible to understand not only the chemical composition of the SEI film but also the distribution of each element on the electrode surface, thus making it possible to understand the side reactions and the role of each individual solvent in PIBs. This could guide us toward strategies for more effective electrolyte optimization.

Battery safety

Safety problems remain a huge concern for LIBs, although they have been successfully commercialized in the past decades (*91*). Their organic flammable electrolytes intrinsically pose safety threats during cycling, and the possibility of thermal runaway is considered to be the main issue that induces safety concern (*96*, *97*). Thermal runaway studies of the K-graphite system indicate that it will go into thermal runaway at a lower temperature and generate less heat compared to the commercial Li-graphite anodes. On the basis of the research experience on LIBs, efforts should be focused on combining theoretical and experimental evidence to monitor the temperature distribution inside the batteries. Specifically, three possible ways could address the safety concerns of PIBs: (i) thermally stable and low-cost separators with high melting points; (ii) solid electrolytes and quasi-solid electrolytes such as polymer-based electrolytes, which will lower the risks of internal short circuits and thermal explosions; and (iii) liquid electrolytes or electrode materials with flame retardants as additives to increase the thermal activation temperature.

Full-cell design

To approach the practical application and commercialization of electrode materials, full-cell fabrication or research is necessary. It is relatively difficult to fabricate full-cell PIBs because fabrication always needs to be based on clear reaction mechanisms and careful calculation/pairing for each electrode (cathode and anode). Although some pioneering work regarding full PIBs has been reported {such as PB//Bi, PB//Super P, $K_{0.7}Fe_{0.5}Mn_{0.5}O_2$//soft carbon, N-content-doped porous carbon monolith//perylene-3,4,9,10-tetracarboxylic dianhydride (PNCM//PTCDA), and graphite//$K_2Mn[Fe(CN)_6]$} with reasonable capacity, and some of these batteries have had higher energy and power densities than full SIBs, the required energy output and long-term cycling stability leave them far away from practical application. Further research on full-cell PIBs will place an emphasis on the full-cell fabrication technology as well as the electrochemical mechanisms and optimization of each individual electrode in the full-cell system.

High-throughput computational design and simulations

High-throughput computational materials design relies on first-principles methods with the aim of calculating the properties of materials in advance of synthesis by solving the basic equations of quantum mechanics and statistical mechanics (*98*, *99*). It is challenging to explore excellent electrode materials, taking into account all of its aspects, including cost, safety, capacity, diffusion kinetics, cycling stability, and suitable electrolytes, which may be hard to evaluate due to the strict experimental conditions. This computational screening method can be carried out on the basis of performing ab initio calculations on candidate materials with a few physical parameters to solve the electronic structure problems, making it possible to address all the abovementioned problems at the same time. Furthermore, especially in the initial stage of research on PIBs, it is meaningful to establish a reliable database to offer guidelines to enable efficient searching for candidate electrode materials and electrolytes, which would be beneficial for simplifying the subsequent experimental procedures and costs.

In summary, the PIB system is emerging as a great candidate for large-scale energy storage, although it is unlikely that all the problems in PIB research can be addressed at the same time. Therefore, summarizing all possible strategies to provide an in-depth perspective will be necessary to make the PIBs viable in the future.

REFERENCES AND NOTES

1. B. Dunn, H. Kamath, J.-M. Tarascon, Electrical energy storage for the grid: a battery of choices. *Science* **334**, 928–935 (2011).
2. B. Kang, G. Ceder, Battery materials for ultrafast charging and discharging. *Nature* **458**, 190–193 (2009).
3. N. Yabuuchi, K. Kubota, M. Dahbi, S. Komaba, Research development on sodium-ion batteries. *Chem. Rev.* **114**, 11636–11682 (2014).
4. H. Kim, J. C. Kim, M. Bianchini, D.-H. Seo, J. Rodriguez-Garcia, G. Ceder, Recent progress and perspective in electrode materials for K-ion batteries. *Adv. Energy Mater.* **8**, 1702384 (2018).
5. X. Wu, D. P. Leonard, X. Ji, Emerging non-aqueous potassium-ion batteries: Challenges and opportunities. *Chem. Mater.* **29**, 5031–5042 (2017).
6. C. Vaalma, D. Buchholz, M. Weil, S. Passerini, A cost and resource analysis of sodium-ion batteries. *Nat. Rev. Mater.* **3**, 18013 (2018).
7. K. Kubota, M. Dahbi, T. Hosaka, S. Kumakura, S. Komaba, Towards K-ion and Na-ion batteries as "Beyond Li-ion". *Chem. Rec.* **18**, 459–479 (2018).
8. T. A. Pham, K. E. Kweon, A. Samanta, V. Lordi, J. E. Pask, Solvation and dynamics of sodium and potassium in ethylene carbonate from ab initio molecular dynamics simulations. *J. Phys. Chem. C* **121**, 21913–21920 (2017).
9. Y. Liu, Z. Tai, J. Zhang, W. K. Pang, Q. Zhang, H. Feng, K. Konstantinov, Z. Guo, H. K. Liu, Boosting potassium-ion batteries by few-layered composite anodes prepared via solution-triggered one-step shear exfoliation. *Nat. Commun.* **9**, 3645 (2018).
10. Z. Jian, W. Luo, X. Ji, Carbon electrodes for K-ion batteries. *J. Am. Chem. Soc.* **137**, 11566–11569 (2015).
11. W. Zhang, W. K. Pang, V. Sencadas, Z. Guo, Understanding high-energy-density Sn_4P_3 anodes for potassium-ion batteries. *Joule* **2**, 1534–1547 (2018).
12. W. Zhang, J. Mao, S. Li, Z. Chen, Z. Guo, Phosphorus-based alloy materials for advanced potassium-ion battery anode. *J. Am. Chem. Soc.* **139**, 3316–3319 (2017).
13. S. Komaba, T. Hasegawa, M. Dahbi, K. Kubota, Potassium intercalation into graphite to realize high-voltage/high-power potassium-ion batteries and potassium-ion capacitors. *Electrochem. Commun.* **60**, 172–175 (2015).

14. Q. Zhao, Y. Hu, K. Zhang, J. Chen, Potassium–sulfur batteries: A new member of room-temperature rechargeable metal–sulfur batteries. *Inorg. Chem.* **53**, 9000–9005 (2014).
15. Y. Liu, Z. Tai, Q. Zhang, H. Wang, W. K. Pang, H. K. Liu, K. Konstantinov, Z. Guo, A new energy storage system: Rechargeable potassium-selenium battery. *Nano Energy* **35**, 36–43 (2017).
16. X. Ren, Y. Wu, A low-overpotential potassium–oxygen battery based on potassium superoxide. *J. Am. Chem. Soc.* **135**, 2923–2926 (2013).
17. R. A. Adams, A. Varma, V. G. Pol, Mechanistic elucidation of thermal runaway in potassium-ion batteries. *J. Power Sources* **375**, 131–137 (2018).
18. P. G. Bruce, S. A. Freunberger, L. J. Hardwick, J.-M. Tarascon, Li–O_2 and Li–S batteries with high energy storage. *Nat. Mater.* **11**, 19–29 (2012).
19. P. G. Bruce, B. Scrosati, J.-M. Tarascon, Nanomaterials for rechargeable lithium batteries. *Angew. Chem. Int. Ed.* **47**, 2930–2946 (2008).
20. Z. Xing, Y. Qi, Z. Jian, X. Ji, Polynanocrystalline graphite: A new carbon anode with superior cycling performance for K-ion batteries. *ACS Appl. Mater. Interfaces* **9**, 4343–4351 (2017).
21. D.-S. Bin, Z.-X. Chi, Y. Li, K. Zhang, X. Yang, Y.-G. Sun, J.-Y. Piao, A.-M. Cao, L.-J. Wan, Controlling the compositional chemistry in single nanoparticles for functional hollow carbon nanospheres. *J. Am. Chem. Soc.* **139**, 13492–13498 (2017).
22. K. Share, A. P. Cohn, R. Carter, B. Rogers, C. L. Pint, Role of nitrogen-doped graphene for improved high-capacity potassium ion battery anodes. *ACS Nano* **10**, 9738–9744 (2016).
23. K. Lei, C. Wang, L. Liu, Y. Luo, C. Mu, F. Li, J. Chen, A porous network of bismuth used as the anode material for high-energy-density potassium-ion batteries. *Angew. Chem. Int. Ed. Engl.* **57**, 4687–4691 (2018).
24. N. D. Schuppert, S. Mukherjee, A. M. Bates, E.-J. Son, M. J. Choi, S. Park, Ex-situ X-ray diffraction analysis of electrode strain at TiO_2 atomic layer deposition/α-MoO_3 interface in a novel aqueous potassium ion battery. *J. Power Sources* **316**, 160–169 (2016).
25. J. Zhou, L. Wang, M. Yang, J. Wu, F. Chen, W. Huang, N. Han, H. Ye, F. Zhao, Y. Li, Hierarchical VS_2 nanosheet assemblies: A universal host material for the reversible storage of alkali metal ions. *Adv. Mater.* **29**, 1702061 (2017).
26. H. Gao, T. Zhou, Y. Zheng, Q. Zhang, Y. Liu, J. Chen, H. Liu, Z. Guo, CoS quantum dot nanoclusters for high-energy potassium-ion batteries. *Adv. Funct. Mater.* **27**, 1702634 (2017).
27. C. Yang, J. Feng, F. Lv, J. Zhou, C. Lin, K. Wang, Y. Zhang, Y. Yang, W. Wang, J. Li, Metallic graphene-like VSe_2 ultrathin nanosheets: Superior potassium-ion storage and their working mechanism. *Adv. Mater.* **30**, 1800036 (2018).
28. Y.-H. Zhu, X. Yang, D. Bao, X.-F. Bie, T. Sun, S. Wang, Y.-S. Jiang, X.-B. Zhang, J.-M. Yan, Q. Jiang, High-energy-density flexible potassium-ion battery based on patterned electrodes. *Joule* **2**, 736–746 (2018).
29. C. D. Wessells, S. V. Peddada, R. A. Huggins, Y. Cui, Nickel hexacyanoferrate nanoparticle electrodes for aqueous sodium and potassium ion batteries. *Nano Lett.* **11**, 5421–5425 (2011).
30. X. Wang, X. Xu, C. Niu, J. Meng, M. Huang, X. Liu, Z. Liu, L. Mai, Earth abundant Fe/Mn-based layered oxide interconnected nanowires for advanced K-ion full batteries. *Nano Lett.* **17**, 544–550 (2017).
31. B. Cao, Q. Zhang, H. Liu, B. Xu, S. Zhang, T. Zhou, J. Mao, W. K. Pang, Z. Guo, A. Li, J. Zhou, X. Chen, H. Song, Graphitic carbon nanocage as a stable and high power anode for potassium-ion Batteries. *Adv. Energy Mater.* **8**, 1801149 (2018).
32. Y. Xu, C. Zhang, M. Zhou, Q. Fu, C. Zhao, M. Wu, Y. Lei, Highly nitrogen doped carbon nanofibers with superior rate capability and cyclability for potassium ion batteries. *Nat. Commun.* **9**, 1720 (2018).
33. V. Lakshmi, Y. Chen, A. A. Mikhaylov, A. G. Medvedev, I. Sultana, M. M. Rahman, O. Lev, P. V. Prikhodchenko, A. M. Glushenkov, Nanocrystalline SnS_2 coated onto reduced graphene oxide: Demonstrating the feasibility of a non-graphitic anode with sulfide chemistry for potassium-ion batteries. *Chem. Commun.* **53**, 8272–8275 (2017).
34. K. Xie, K. Yuan, X. Li, W. Lu, C. Shen, C. Liang, R. Vajtai, P. Ajayan, B. Wei, Superior potassium ion storage via vertical MoS_2 "Nano-Rose" with expanded interlayers on graphene. *Small* **13**, 1701471 (2017).
35. Z. Liu, P. Li, G. Suo, S. Gong, W. A. Wang, C.-Y. Lao, Y. Xie, H. Guo, Q. Yu, W. Zhao, K. Han, Q. Wang, M. Qin, K. Xi, X. Qu, Zero-strain $K_{0.6}Mn_1F_{2.7}$ hollow nanocubes for ultrastable potassium ion storage. *Energy Environ. Sci.* **11**, 3033–3042 (2018).
36. G. He, L. F. Nazar, Crystallite size control of prussian white analogues for nonaqueous potassium-ion batteries. *ACS Energy Lett.* **2**, 1122–1127 (2017).
37. K. R. Paton, E. Varrla, C. Backes, R. J. Smith, U. Khan, A. O'Neill, C. Boland, M. Lotya, O. M. Istrate, P. King, T. Higgins, S. Barwich, P. May, P. Puczkarski, I. Ahmed, M. Moebius, H. Pettersson, E. Long, J. Coelho, S. E. O'Brien, E. K. McGuire, B. M. Sanchez, G. S. Duesberg, N. McEvoy, T. J. Pennycook, C. Downing, A. Crossley, V. Nicolosi, J. N. Coleman, Scalable production of large quantities of defect-free few-layer graphene by shear exfoliation in liquids. *Nat. Mater.* **13**, 624–630 (2014).
38. Z. Tai, C. M. Subramaniyam, S. L. Chou, L. Chen, H.-K. Liu, S.-X. Dou, Few atomic layered lithium cathode materials to achieve ultrahigh rate capability in lithium-ion batteries. *Adv. Mater.* **29**, 1700605 (2017).
39. G. Niu, L. Zhang, A. Ruditskiy, L. Wang, Y. Xia, A droplet-reactor system capable of automation for the continuous and scalable production of noble-metal nanocrystals. *Nano Lett.* **18**, 3879–3884 (2018).
40. I. Sultana, M. M. Rahman, Y. Chen, A. M. Glushenkov, Potassium-ion battery anode materials operating through the alloying–dealloying reaction mechanism. *Adv. Funct. Mater.* **28**, 1703857 (2018).
41. C. Zeng, F. Xie, X. Yang, M. Jaroniec, L. Zhang, S.-Z. Qiao, Ultrathin titanate nanosheets/graphene films derived from confined transformation for excellent Na/K ion storage. *Angew. Chem. Int. Ed. Engl.* **57**, 8540–8544 (2018).
42. X. Wang, G. Sun, P. Routh, D.-H. Kim, W. Huang, P. Chen, Heteroatom-doped graphene materials: Syntheses, properties and applications. *Chem. Soc. Rev.* **43**, 7067–7098 (2014).
43. D. Yu, K. Goh, H. Wang, L. Wei, W. Jiang, Q. Zhang, L. Dai, Y. Chen, Scalable synthesis of hierarchically structured carbon nanotube–graphene fibres for capacitive energy storage. *Nat. Nanotechnol.* **9**, 555 (2014).
44. C. Chen, Z. Wang, B. Zhang, L. Miao, J. Cai, L. Peng, Y. Huang, J. Jiang, Y. Huang, L. Zhang, J. Xie, Nitrogen-rich hard carbon as a highly durable anode for high-power potassium-ion batteries. *Energy Storage Mater.* **8**, 161–168 (2017).
45. J. Li, W. Qin, J. Xie, H. Lei, Y. Zhu, W. Huang, X. Xu, Z. Zhao, W. Mai, Sulphur-doped reduced graphene oxide sponges as high-performance free-standing anodes for K-ion storage. *Nano Energy* **53**, 415–424 (2018).
46. Z. Ju, S. Zhang, Z. Xing, Q. Zhuang, Y. Qiang, Y. Qian, Direct synthesis of few-layer F-doped graphene foam and its lithium/potassium storage properties. *ACS Appl. Mater. Interfaces* **8**, 20682–20690 (2016).
47. S. Gong, Q. Wang, Boron-doped graphene as a promising anode material for potassium-ion batteries with a large capacity, high rate performance, and good cycling stability. *J. Phys. Chem. C* **121**, 24418–24424 (2017).
48. M. Chen, W. Wang, X. Liang, S. Gong, J. Liu, Q. Wang, S. Guo, H. Yang, Sulfur/oxygen codoped porous hard carbon microspheres for high-performance potassium-ion batteries. *Adv. Energy Mater.* **8**, 1800171 (2018).
49. Y. Yao, M. Chen, R. Xu, S. Zeng, H. Yang, S. Ye, F. Liu, X. Wu, Y. Yu, CNT interwoven nitrogen and oxygen dual-doped porous carbon nanosheets as free-standing electrodes for high-performance Na-Se and K-Se flexible batteries. *Adv. Mater.* **30**, e1805234 (2018).
50. Y. Lu, J. Chen, Robust self-supported anode by integrating Sb2S3 nanoparticles with S, N-codoped graphene to enhance K-storage performance. *Sci. China Chem.* **60**, 1533–1539 (2017).
51. G. Ma, K. Huang, J.-S. Ma, Z. Ju, Z. Xing, Q.-C. Zhuang, Phosphorus and oxygen dual-doped graphene as superior anode material for room-temperature potassium-ion batteries. *J. Mater. Chem. A* **5**, 7854–7861 (2017).
52. J. Yang, Z. Ju, Y. Jiang, Z. Xing, B. Xi, J. Feng, S. Xiong, Enhanced capacity and rate capability of nitrogen/oxygen dual-doped hard carbon in capacitive potassium-ion storage. *Adv. Mater.* **30**, 1700104 (2018).
53. Q. Zhang, J. Mao, W. K. Pang, T. Zheng, V. Sencadas, Y. Chen, Y. Liu, Z. Guo, Boosting the potassium storage performance of alloy-based anode materials via electrolyte salt chemistry. *Adv. Energy Mater.* **8**, 1703288 (2018).
54. W. Zhang, Z. Wu, J. Zhang, G. Liu, N.-H. Yang, R.-S. Liu, W. K. Pang, W. Li, Z. Guo, Unraveling the effect of salt chemistry on long-durability high-phosphorus-concentration anode for potassium ion batteries. *Nano Energy* **53**, 967–974 (2018).
55. J. Zhao, X. Zou, Y. Zhu, Y. Xu, C. Wang, Electrochemical intercalation of potassium into graphite. *Adv. Funct. Mater.* **26**, 8103–8110 (2016).
56. X. Lin, J. Huang, H. Tan, J. Huang, B. Zhang, $K_3V_2(PO_4)_2F_3$ as a robust cathode for potassium-ion batteries. *Energy Storage Mater.* **16**, 97–101 (2019).
57. W. Yu, K. C. Lau, Y. Lei, R. Liu, L. Qin, W. Yang, B. Li, L. A. Curtiss, D. Zhai, F. Kang, Dendrite-free potassium–oxygen battery based on a liquid alloy anode. *ACS Appl. Mater. Interfaces* **9**, 31871–31878 (2017).
58. A. P. Cohn, N. Muralidharan, R. Carter, K. Share, L. Oakes, C. L. Pint, Durable potassium ion battery electrodes from high-rate cointercalation into graphitic carbons. *J. Mater. Chem. A* **4**, 14954–14959 (2016).
59. N. Xiao, W. D. McCulloch, Y. Wu, Reversible dendrite-free potassium plating and stripping electrochemistry for potassium secondary batteries. *J. Am. Chem. Soc.* **139**, 9475–9478 (2017).
60. J. Liao, Q. Hu, Y. Yu, H. Wang, Z. Tang, Z. Wen, C. Chen, A potassium-rich iron hexacyanoferrate/dipotassium terephthalate@carbon nanotube composite used for K-ion full-cells with an optimized electrolyte. *J. Mater. Chem. A* **5**, 19017–19024 (2017).
61. L. Wang, J. Zou, S. Chen, G. Zhou, J. Bai, P. Gao, Y. Wang, X. Yu, J. Li, Y.-S. Hu, H. Li, TiS_2 as a high performance potassium ion battery cathode in ether-based electrolyte. *Energy Storage Mater.* **12**, 216–222 (2018).
62. S. Sankarasubramanian, V. Ramani, Dimethyl sulfoxide (DMSO)-based electrolytes for high current potassium-oxygen batteries. *J. Phys. Chem. C* **122**, 19319–19327 (2018).
63. J. Huang, X. Lin, H. Tan, B. Zhang, Bismuth microparticles as advanced anodes for potassium-ion battery. *Adv. Energy Mater.* **8**, 1703496 (2018).
64. H. Gao, L. Xue, S. Xin, J. B. Goodenough, A high-energy-density potassium battery with a polymer-gel electrolyte and a polyaniline cathode. *Angew. Chem.* **130**, 5547–5551 (2018).

65. T. Yamamoto, K. Matsumoto, R. Hagiwara, T. Nohira, Physicochemical and electrochemical properties of K[$N(SO_2F)_2$]–[*N*-methyl-*N*-propylpyrrolidinium][$N(SO_2F)_2$] ionic liquids for potassium-ion batteries. *J. Phys. Chem. C* **121**, 18450–18458 (2017).
66. M. D. Slater, D. Kim, E. Lee, C. S. Johnson, Sodium-ion batteries. *Adv. Funct. Mater.* **23**, 947–958 (2013).
67. W. Zhang, J. Mao, W. K. Pang, X. Wang, Z. Guo, Creating fast ion conducting composites via in-situ introduction of titanium as oxygen getter. *Nano Energy* **49**, 549–554 (2018).
68. Q. Wang, W. Zhang, C. Guo, Y. Liu, C. Wang, Z. Guo, In situ construction of 3D interconnected FeS@Fe_3C@graphitic carbon networks for high-performance sodium-ion Batteries. *Adv. Funct. Mater.* **27**, 1703390 (2017).
69. Z. Tai, Y. Liu, Q. Zhang, T. Zhou, Z. Guo, H. K. Liu, S. X. Dou, Ultra-light and flexible pencil-trace anode for high performance potassium-ion and lithium-ion batteries. *Green Energy Environ.* **2**, 278–284 (2017).
70. Y. Liu, W. Wang, J. Wang, Y. Zhang, Y. Zhu, Y. Chen, L. Fu, Y. Wu, Sulfur nanocomposite as a positive electrode material for rechargeable potassium–sulfur batteries. *Chem. Commun.* **54**, 2288–2291 (2018).
71. J.-Y. Hwang, H. M. Kim, C. S. Yoon, Y.-K. Sun, Toward high-safety potassium–sulfur batteries using a potassium polysulfide catholyte and metal-free anode. *ACS Energy Lett.* **3**, 540–541 (2018).
72. X. Lu, M. E. Bowden, V. L. Sprenkle, J. Liu, A low cost, high energy density, and long cycle life potassium–sulfur battery for grid-scale energy storage. *Adv. Mater.* **27**, 5915–5922 (2015).
73. N. Xiao, X. Ren, W. D. McCulloch, G. Gourdin, Y. Wu, Potassium superoxide: A unique alternative for metal–air batteries. *Acc. Chem. Res.* **51**, 2335–2343 (2018).
74. W. Wang, N.-C. Lai, Z. Liang, Y. Wang, Y.-C. Lu, Superoxide stabilization and a universal KO_2 growth mechanism in potassium–oxygen batteries. *Angew. Chem.* **130**, 5136–5140 (2018).
75. K. Lu, H. Zhang, F. Ye, W. Luo, H. Ma, Y. Huang, Rechargeable potassium-ion batteries enabled by potassium-iodine conversion chemistry. *Energy Storage Mater.* **16**, 1–5 (2019).
76. Q. Zou, Z. Liang, G.-Y. Du, C.-Y. Liu, E. Y. Li, Y.-C. Lu, Cation-directed selective polysulfide stabilization in alkali metal–sulfur batteries. *J. Am. Chem. Soc.* **140**, 10740–10748 (2018).
77. X. Yu, A. Manthiram, A reversible nonaqueous room-temperature potassium-sulfur chemistry for electrochemical energy storage. *Energy Storage Mater.* **15**, 368–373 (2018).
78. N. Xiao, R. T. Rooney, A. A. Gewirth, Y. Wu, The long-term stability of KO_2 in K-O_2 batteries. *Angew. Chem.* **130**, 1241–1245 (2018).
79. W. Ren, X. Chen, C. Zhao, Ultrafast aqueous potassium-ion batteries cathode for stable intermittent grid-scale energy storage. *Adv. Energy Mater.* **8**, 1801413 (2018).
80. D. Su, A. McDonagh, S.-Z. Qiao, G. Wang, High-capacity aqueous potassium-ion batteries for large-scale energy storage. *Adv. Mater.* **29**, 1604007 (2017).
81. D. P. Leonard, Z. Wei, G. Chen, F. Du, X. Ji, A water-in-salt electrolyte for potassium-ion batteries. *ACS Energy Lett.* **3**, 373–374 (2018).
82. L. Fan, K. Lin, J. Wang, R. Ma, B. Lu, A nonaqueous potassium-based battery–supercapacitor hybrid device. *Adv. Mater.* **30**, 1800804 (2018).
83. J. Zhu, Y. Li, B. Yang, L. Liu, J. Li, X. Ya, D. He, A dual carbon-based potassium dual ion battery with robust comprehensive performance. *Small* **14**, 1801836 (2018).
84. B. Ji, F. Zhang, X. Song, Y. Tang, A novel potassium-ion-based dual-ion battery. *Adv. Mater.* **29**, 1700519 (2017).
85. J. Zheng, W. Deng, Z. Hu, Z. Zhuo, F. Liu, H. Chen, Y. Lin, W. Yang, K. Amine, R. Li, J. Lu, F. Pan, Asymmetric K/Li-ion battery based on intercalation selectivity. *ACS Energy Lett.* **3**, 65–71 (2018).
86. L. Fan, Q. Liu, S. Chen, K. Lin, Z. Xu, B. Lu, Potassium-based dual ion battery with dual-graphite electrode. *Small* **13**, 1701011 (2017).
87. R. Lian, D. Wang, X. Ming, R. Zhang, Y. Wei, J. Feng, X. Meng, G. Chen, Phase transformation, ionic diffusion, and charge transfer mechanisms of $KVOPO_4$ in potassium ion batteries: First-principles calculations. *J. Mater. Chem. A* **6**, 16228–16234 (2018).
88. A. Y. Galashev, A. S. Vorob'ev, Physical properties of silicene electrodes for Li-, Na-, Mg-, and K-ion batteries. *J. Solid State Electrochem.* **22**, 3383–3391 (2018).
89. P. Bhauriyal, A. Mahata, B. Pathak, Graphene-like carbon–nitride monolayer: A potential anode material for Na- and K-ion batteries. *J. Phys. Chem. C* **122**, 2481–2489 (2018).
90. H. D. Yoo, E. Markevich, G. Salitra, D. Sharon, D. Aurbach, On the challenge of developing advanced technologies for electrochemical energy storage and conversion. *Mater. Today* **17**, 110–121 (2014).
91. N. Nitta, F. Wu, J. T. Lee, G. Yushin, Li-ion battery materials: Present and future. *Mater. Today* **18**, 252–264 (2015).
92. C. Yan, Y.-X. Yao, X. Chen, X.-B. Cheng, X.-Q. Zhang, J.-Q. Huang, Q. Zhang, Lithium nitrate solvation chemistry in carbonate electrolyte sustains high-voltage lithium metal batteries. *Angew. Chem.* **130**, 14251–14255 (2018).
93. H. Zhang, G. G. Eshetu, X. Judez, C. Li, L. M. Rodriguez-Martínez, M. Armand, Electrolyte additives for lithium metal anodes and rechargeable lithium metal batteries: Progresses and perspectives. *Angew. Chem. Int. Ed.* **57**, 15002–15027 (2018).
94. F.-Q. Liu, W.-P. Wang, Y.-X. Yin, S.-F. Zhang, J.-L. Shi, L. Wang, X.-D. Zhang, Y. Zheng, J.-J. Zhou, L. Li, T.-G. Guo, Upgrading traditional liquid electrolyte via in situ gelation for future lithium metal batteries. *Sci. Adv.* **4**, eaat5383 (2018).
95. Y. Li, W. Huang, Y. Li, A. Pei, D. T. Boyl, Y. Cui, Correlating structure and function of battery interphases at atomic resolution using cryoelectron microscopy. *Joule* **2**, 2167–2177 (2018).
96. K. Liu, Y. Liu, D. Lin, A. Pei, Y. Cui, Materials for lithium-ion battery safety. *Sci. Adv.* **4**, eaas9820 (2018).
97. X. Liu, D. Ren, H. Hsu, X. Feng, G. L. Xu, M. Zhuang, H. Gao, L. Lu, X. Han, Z. Chu, J. Li, X. He, K. Amine, M. Ouyang, Thermal runaway of lithium-ion batteries without internal short circuit. *Joule* **2**, 2047–2064 (2018).
98. G. Hautier, A. Jain, S. P. Ong, B. Kang, C. Moore, R. Doe, G. Ceder, Phosphates as lithium-ion battery cathodes: An evaluation based on high-throughput ab initio calculations. *Chem. Mater.* **23**, 3495–3508 (2011).
99. S. Curtarolo, G. L. W. Hart, M. B. Nardelli, N. Mingo, S. Sanvito, O. Levy, The high-throughput highway to computational materials design. *Nat. Mater.* **12**, 191–201 (2013).
100. B. Ji, F. Zhang, N. Wu, Y. Tang, A dual-carbon battery based on potassium-ion electrolyte. *Adv. Energy Mater.* **7**, 1700920 (2017).

Acknowledgments: We thank our colleagues for their contributions to the work cited. We also thank T. Silver for performing critical revision of the manuscript. **Funding:** This research has been conducted with the support of an Australian Government Research Training Program Scholarship (Y.L.) and financial support provided by the University of Wollongong (W.Z.). Support from the Australian Research Council through Future Fellowship and Discovery projects (FT150100109, FT160100251, and DP170102406) is gratefully acknowledged. **Author contributions:** All authors contributed to discussions of the content and conceived the topic of the Review. W.Z. and Y.L. co-wrote the manuscript and prepared the figures. Z.G. edited and reviewed the article before submission. **Competing interests:** The authors declare that they have no competing interests. **Data and materials availability:** All data needed to evaluate the conclusions in the paper are present in the paper and/or the materials cited herein. Additional data related to this paper may be requested from the authors.

Submitted 1 November 2018
Accepted 1 April 2019
Published 10 May 2019
10.1126/sciadv.aav7412

Citation: W. Zhang, Y. Liu, Z. Guo, Approaching high-performance potassium-ion batteries via advanced design strategies and engineering. *Sci. Adv.* **5**, eaav7412 (2019).